LAWRENCE
LIVERMORE
NATIONAL
LABORATORY

UCRL-JRNL-221430

Experimental and Numerical Studies of Separatrix Splitting and Magnetic Footprints in DIII-D

T.E. Evans, I. Joseph, R.A. Moyer, M.E. Fenstermacher, C.J. Lasnier, L. Yan

May 17, 2006

Journal of Nuclear Materials

Disclaimer

Experimental and numerical studies of separatrix splitting and magnetic footprints in DIII-D∴

T. E. Evans[a*], **I. Joseph**[b], R. A. Moyer[b], M. E. Fenstermacher[c], C. J. Lasnier[c], and L. Yan[d]

[a]*General Atomics, P.O. Box 85608, San Diego, CA, 92186-5608, USA*

[b]*University of California at San Diego, 9500 Gillman Drive, La Jolla, CA, 92093, USA*

[c]*Lawrence Livermore National Laboratory, Livermore, California USA*

[d]*Southwestern Institute of Physics, P. O. Box 432, Chengdu, Sichuan, China*

A numerical field line integration code is used to study the structure of divertor footprints produced by small non-axisymmetirc magnetic perturbation in the DIII-D tokamak. The numerical modeling results are compared to experimental infrared camera data which show a splitting of the divertor target plate heat flux into several distinct peaks when an n=3 magnetic perturbation from the DIII-D I-coil is applied. The heat flux splitting consistently appears when the n=3 perturbation is applied and disappears when the perturbation is removed. The magnitude of the splitting implied by the numerical modeling is a factor of 3 smaller than the splitting seen in the experimental data. These results suggest that the plasma response to the edge resonant applied n=3 magnetic perturbation produces an amplification of the vacuum magnetic footprint structure on the divertor target plates. These results may have significant implications for the ITER divertor design.

∴**Keywords:** DIII-D, Edge modeling, ELM, Magnetic Topology, Stochastic boundary

PACS: 05.45.-a, 05.45.Pq, 28.52.-s, 52.55.Fa, 52.55.-s, 52.55.Rk, 52.25.Fi

*Corresponding author: General Atomics, P.O. Box 85608, San Diego, CA 92186 USA

e-mail: evans@fusion.gat.com

Presenting author and e-mail: I. Joseph, josephi@fusion.gat.com

1. Introduction

When subjected to small non-axisymmetric magnetic perturbations, the separatrix of a poloidally diverted tokamak is transformed from an axisymmetric 2D geometry into a set of intersecting invariant manifolds that define a somewhat more complex 3D topology [1]. We refer to this process as separatrix splitting and the patterns formed by the intersection of the invariant manifolds with solid surfaces as magnetic footprints. This process is unavoidable when non-axisymmetric magnetic perturbations, such as those from external correction/control coils, field-errors or internal MHD modes, are present in the system although the plasma response may act to amplify or reduce this effect. These magnetic structures can have significant implications for the deposition of heat and particle fluxes on divertor structures and first wall components and thus are of considerable interest for plasma-surface interaction research in toroidal fusion devices.

The mathematical theory of the structures formed due to separatrix or invariant manifold splitting in simple Hamiltonian systems, generically referred to as homoclinic tangles, has been extensively studied and although quite complex is relatively well understood [2-4]. The application of invariant manifold theory to magnetic field lines in realistic poloidally diverted tokamaks is most directly facilitated by using numerical field line integration and mapping codes such as TRIP3D [4] and TRIP3D_MAP [5] where the unperturbed axisymmetric field is derived from experimentally constrained equilibria, calculated with the EFIT Grad-Shafranov code [6], that includes the effects of the plasma pressure and current density. In addition, mapping codes used to study simplified wire models of poloidally diverted tokamaks [7] are valuable for comparing the properties of

field line trajectories to a broader class generic behaviors defined by the dynamics of conservative vector fields Hamiltonian systems.

In this paper we present experimental measurements of heat flux and particle recycling patterns in the DIII-D lower divertor that are, as best we can determine, consistent with the expected structure of magnetic footprints defined by homoclinic tangles produced an applied n=3 magnetic perturbation from the DIII-D I-coil [8]. The experimental data is presented in Section 2 and the numerical modeling of the magnetic footprints, calculated with the TRIP3D field line integration code, is presented in Section 3. This is followed by a discussion of the comparisons between the experimental measurements and the numerical modeling and conclusions in Section 4.

2. Experimental background and observations

The separatrix splitting and magnetic footprint studies discussed in this paper are done using target plate imaging diagnostics located at two toroidal angles that view the lower DIII-D divertor of a double null plasma biased downward by 20 mm as shown in Fig. 1a (discharge 115467). The principle diagnostics are an IRTV [9] centered at a toroidal angle $\phi = 60^{o}$, as shown in Fig. 1a, and a downward tilted, tangentially aligned visible camera viewing D_{α} recycling light between $\phi = 120^{o}$ and $\phi = 225^{o}$ [10]. The IRTV system is used to measure the radial heat flux profile across the lower divertor as a function of time. A typical heat flux profile during an ELMing H-mode with no externally imposed resonant magnetic perturbations, other than intrinsic field-errors, is show along the lower divertor tiles in Fig. 1a. The D_{α} camera provides 3D (R, z, ϕ) images of the lower divertor recycling at 16.7 ms intervals through the discharge. Figure 1b shows the

poloidal structure of the split separatrix at $\phi = 60^{o}$ calculated using TRIP3D_MAP during an n=3 I-coil pulse. This calculation is done using the methods described in Refs. 1 and 5.

The key plasma parameters for this discharge are the: elongation (k) of 1.8, upper and lower triangularities of 0.35 and 0.73 respectively, toroidal magnetic field B_T = 1.6T, plasma current I_p = 1.1 MA and neutral beam heating power of 5.1 MW. The normalized Greenwald electron pedestal density density ($n_{eG\text{-}ped}$) was 0.55 with a line average density (n_e) of 7.2×10^{19} m^{-3}. An L-H transition occurred at t = 1600 ms and established regular type-I ELMs within the first 300-400 ms of the L-H transition. The normalized plasma pressure (β_N) was 2.2 and the H_{L89} confinement quality factor is 2.1. The safety factor at the 95% flux surface (q_{95}) ranged between 3.4 and 4.1. In this discharge an n=3 I-coil pulse was used to suppress ELMs [8] and the DIII-D C-coil was not used. The properties of the discharges during the ELM suppressed phases along with various diagnostic responses to the I-coil pulse are discussed extensively in Refs. 8 and 11.

Data collected with the IRTV shows a distinct change in the divertor heat flux at the beginning of the I-coil current pulse followed by the formation of two distinct peaks that are slowly modulated between single and double peak formations during the remainder of the pulse. This temporal evolution of the divertor heat flux across the outer strike point region is represented using as a contour lines in Fig. 2a. Here, red indicating a heat flux of approximately 20 W/cm^2 with each additional contour line representing a change of 5 W/cm^2. A 4.4 kA, n = 3, I-coil current pulse is initiated at 3.0 s and terminates at 4.4 s. The heat flux profile evolves from a single peaked structure at t = 2.9 s, as shown by the green “I-coil off” profile in Fig. 2b, to a double peaked profile at t = 3.3 s with the “I-coil

on" as shown by the red dashed profile in Fig. 2b. The maximum peak-to-peak separations of the double peak formation is 55 mm.

A splitting of the D_α recycling emission near the outer strike point is also seen when the I-coil is pulsed in this discharge. Figure 3 shows the D_α TV view 60 ms after the initiation of the I-coil pulse. The radial resolution of the camera image at the toriodal tangency point with the outer strike point (ϕ = 195º) is 5 mm in this view. Two independent methods have been used to estimate the peak-to-peak splitting of the recycling in this image. This give a range of between 20 and 30 mm at ϕ = 195º. In addition the full width of each peak is estimated to be between 10 and 20 mm.

3. Numerical modeling

Numerical modeling of the magnetic footprint near the out strike point before the I-coil pulse is applied in discharge 115467 show a small n=1 split peak pattern ϕ = 195º with a peak-to-peak separation of approximately 5 mm as seen in Fig. 4. This splitting is due to measured to non-axisymmetric intrinsic field-error components generated by the vertical field coils (DIII-D f-coils), the toroidal field coil bus bars and the toroidal field coil center post legs. The TRIP3D code uses engineering quality models of the known field-errors and perturbation coils (i.,e., the C- and I-coils) in DIII-D to calculate magnetic vector field components needed for field line integration studies [4]. The data shown in Fig. 4 is composed of field lines that were started from 180 uniformly distributed poloidal points on 10 unperturbed normalized flux surface between 0.98 and 0,998 and 8 uniformly distributed toroidal angles. Each field line is integrated in one toroidal direction (in this case the same direction as the toroidal field) for 200 toroidal transits or until is strikes the lower divertor target plate where its (R, ϕ) position is recorded with a dot and its flux

surface of origin is designated by the color of the dot used with red to blue corresponding to 0.98 to 0.998 respectively.

When the I-coil pulses in discharge 115467 the magnetic footprint calculated with TRIP3D form a clear n=3 structure while the total width of the structure at $\phi = 195^{o}$ remains approximately constant as seen in Fig. 5. At the toroidal location of the IRTV ($\phi = 60^{o}$ indicated by the red line in Figs. 4 and 5) 3 new radial stripes with peak-to-peak separations of 2 mm, 5 mm and 9 mm appear. The tips of these stripes have a much lower field line hit point density than the stems from which they emanate and are dominated by field lines from deeper flux surfaces.

4. Discussion and conclusions

A comparison of the experimental data, during the I-coil pulse as shown in Figs. 2 and 3, with the numerical calculations of the magnetic footprint near outer strike point (Fig. 5) indicates that a non-axisymmetric splitting of the separatrix is qualitatively consistent with the experimental data. Since the structure appears in both the heat flux profile at $\phi = 60^{o}$ and in the D_{α} images at $\phi = 195^{o}$ when the I-coil pulse is initiated and disappear when the I-coil pulse terminates it is clearly correlated with the applied n=3 magnetic perturbation. Similar features have been seen during locked modes, ELMs and disruptions in DIII-D [12].

Quantitative estimates of the peak-to-peak splitting in the heat flux profile indicate two peaks separated by 55 mm while the numerical results indicate a total of 4 discrete stripes separated by 2, 5 and 9 mm from inner to outer respectively. Since the spatial resolution of the IRTV is of order 15 mm the fine structure predicted by the modeling is not be visible in the data. Nevertheless, the data and the modeling taken together suggest

that the applied perturbation may be amplified by as much a factor of 5-6 by plasma effects. Interestingly, at the D_α imaging location the numerical modeling results indicate a peak-to-peak splitting of about 5-8 mm during the I-coil pulse and the experimental data shows a 20-30 mm split which would be consistent a factor of 4-5 amplification. Additionally, the decrease seen in the experimental peak-to-peak separation from $\phi = 60^o$ to $\phi = 195^o$ is qualitatively consistent with the numerical results shown in Fig. 5.

These results demonstrate that heat and particle deposition patterns seen on the target plates of a poloidally diverted plasma are qualitatively consistent with the magnetic footprints produced by a splitting of the separatrix when small non-axisymmetric magnetic perturbations are present in the system. In addition, the experimental data presented here indicates that the plasma response amplifies the magnitude of the splitting by as much as a factor of 6. Since small non-axisymmetric perturbations are commonplace in toroidal magnetic confinement systems, separatrix splitting when combined with the potential for large amplification factors due to the plasma response can have significant implications for the design of power and particle handling components in burning plasma devices such as ITER.

5. Acknowledgements

Work performed under the auspices of the US DOE by UC, LLNL under Contract W-7405-ENG-48. DE-FG02-05ER54809, DE-FG02-04ER54758, and DE-FC02-04ER54698.

7. References

[1] T. E. Evans, R. K. W. Roeder, J. A. Carter, et al., *J. Phys.: Conf. Ser.* **7** (2005) 174.

[2] J. Guckenheimer and P. Holmes, *Nonlinear Oscillations, Dynamical Systems, and Bifurcations of Vector Fields* Applied Mathematical Science **42** (New York: Springer-Verlag) 1983.

[3] V. K. Melnikov, *Transactions of Moscow Mathematical Society* **12** (1963) 1.

[4] J. D. Meiss, *Rev. Mod. Phys.* **64** (1992) 795.

[4] T. E. Evans, R. A. Moyer and P. Monat, *Phys. Plasmas* **9** (2002) 4957.

[5] R. K. W. Roeder, B. I. Rapoport and T. E. Evans, *Phys. Plasmas* **10** (2003) 3796.

[6] L. L. Lao, H. E. St. John, R. D. Stambaugh, et al., *Nucl. Fusion* **25** (1985) 1611.

[7] S. S. Abdullaev, K. H. Finken, M. Jakubowski and M. Lehnen, *Nucl. Fusion* **46** (2006) s113.

[8] T. E. Evans, R. A. Moyer, P.R. Thomas, et al., *Phys. Rev. Lett.* **92** (2004) 235003-1.

[9] C. J. Lasnier, et al.,

[10] M. E. Fenstermacher, et al.,

[11] T. E. Evans, R. A. Moyer, J. G. Watkins, et al., *Nucl. Fusion* **45** (2005) 595.

[12] T. E. Evans, C. J. Lasnier, D. N. Hill, et al., *J. Nucl. Mat.* **220 - 222** (1995) 235.

Figure captions

Fig. 1 (a) DIII-D axisymmetric equilibrium during discharge 115467 showing the IRTV camera view at $\phi = 60^{o}$ and a typical heat flux profile before the I-coil (black dots) is pulsed, (b) typical non-axisymmetric seperatrix structure during the I-coil pulse.

Fig. 2 (a) Contour plot showing the radial distribution of the lower divertor heat flux near the outer strike point (R=1.31 m) as a function of time in discharge 115467. The I-coil is pulsed to 4.4 kA between 3.0 s and 4.4 s, (b) radial heat flux profiles just before (2.9 s) and during (3.3 s) the I-coil pulse.

Fig. 3 Lower divertor recycling emission (D_{α}) during the I-coil pulse in discharge 115467.

Fig. 4 Magnetic footprint calculated with TRIP3D showing field line strike point locations in (R, ϕ) due to DIII-D field-errors only (before the I-coil is pulsed) in discharge 115467.

Fig. 5 The same as Fig. 4 except with the 4.4 kA n=3 I-coil pulse in discharge 115467.

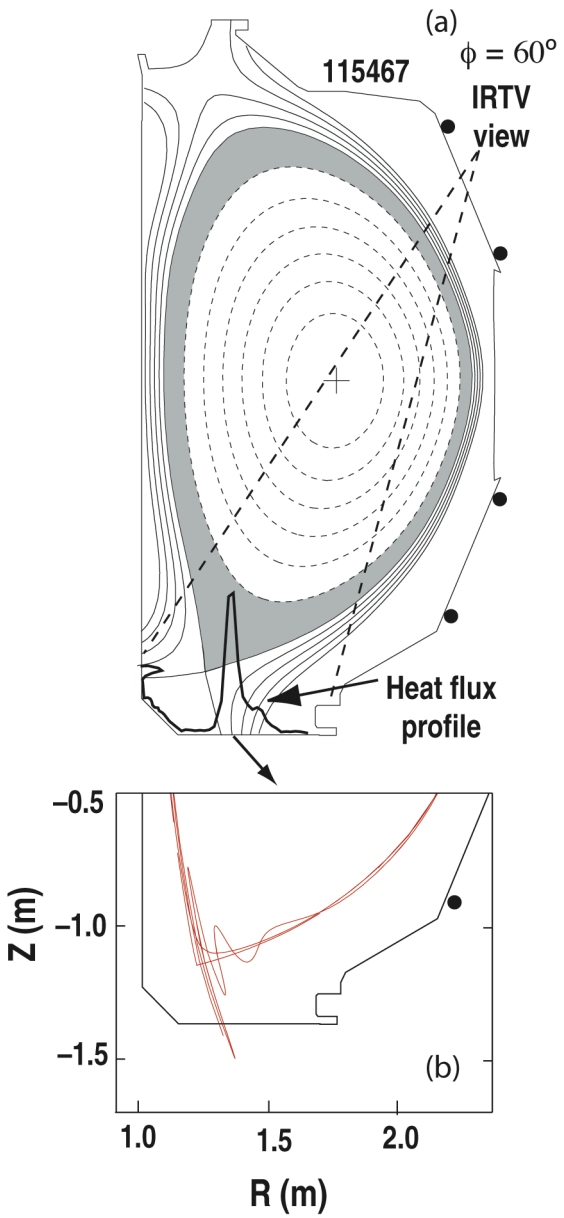

Fig. 1 Evans
75 mm x 161 mm

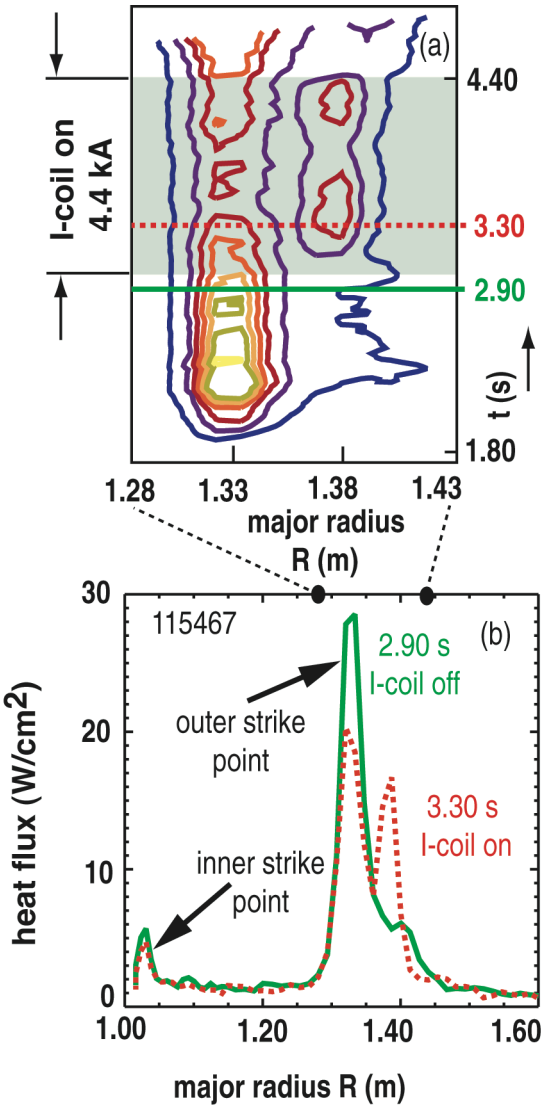

Fig. 2 Evans
75 mm x 145 mm

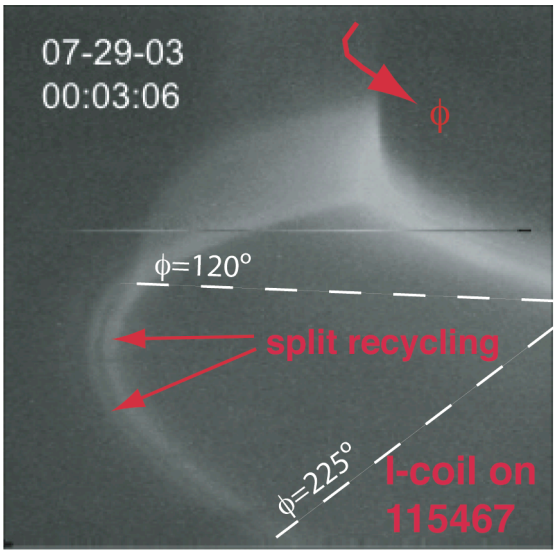

Fig. 3 Evans
75 mm x 72 mm

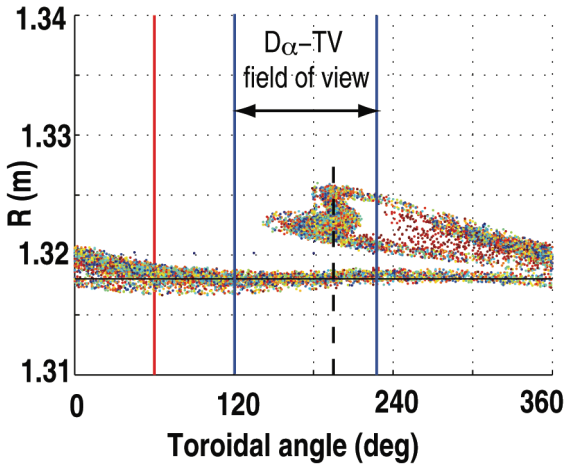

Fig. 4 Evans
75 mm x 62 mm

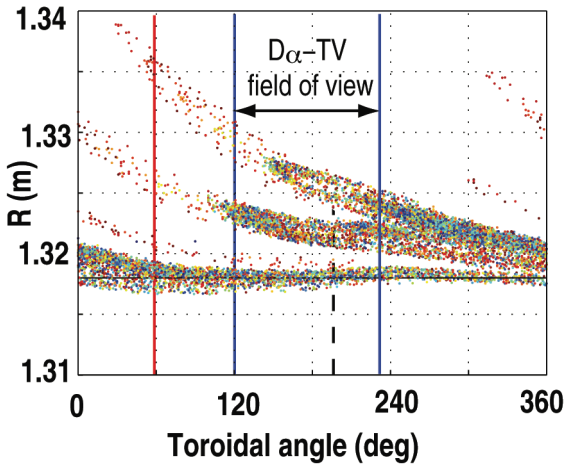

Fig. 5 Evans
75 mm x 62 mm